Astronomy
&
Astrophysics

INTEGRAL-RXTE observations of Cygnus X-1[*]

K. Pottschmidt[1,2], J. Wilms[3], M. Chernyakova[2,4], M. A. Nowak[5], J. Rodriguez[2,6], A. A. Zdziarski[7],
V. Beckmann[2,3], P. Kretschmar[1,2], T. Gleissner[3], G. G. Pooley[8], S. Martínez-Núñez[9,10],
T. J.-L. Courvoisier[2,11], V. Schönfelder[1], and R. Staubert[3]

[1] Max-Planck-Institut für extraterrestrische Physik, Postfach 1312, 85748 Garching, Germany
[2] INTEGRAL Science Data Centre, Chemin d'Écogia 16, 1290 Versoix, Switzerland
[3] Institut für Astronomie und Astrophysik – Abt. Astronomie, Universität Tübingen, Sand 1, 72076 Tübingen, Germany
[4] Astro Space Center of the PN Lebedev Physical Institute, 84/32 Profsoyuznaya Street, Moscow 117997, Russia
[5] MIT-CXC, NE80-6077, 77 Massachusetts Ave., Cambridge, MA 02139, USA
[6] DSM/DAPNIA/Service d'Astrophysique (CNRS FRE 2591), CEA Saclay, 91191 Gif-sur-Yvette, France
[7] Nicolaus Copernicus Astronomical Center, Bartycka 18, 00-716 Warszawa, Poland
[8] Astrophysics, Cavendish Laboratory, Madingley Road, Cambridge CB3 0HE, UK
[9] GACE, Instituto de Ciencia de los Materiales, Universidad de Valencia, PO Box 22085, 46071 Valencia, Spain
[10] Danish Space Research Institute, Juliane Maries Vej 30, 2100 Copenhagen Ø., Denmark
[11] Observatoire de Genève, Chemin des Maillettes 51, 1290 Sauverny, Switzerland

Abstract. We present first results from contemporaneous observations of Cygnus X-1 with *INTEGRAL* and *RXTE*, made during *INTEGRAL*'s performance verification phase in 2002 November and December. Consistent with earlier results, the $3-250$ keV data are well described by Comptonization spectra from a Compton corona with a temperature of $kT \sim 50-90$ keV and an optical depth of $\tau \sim 1.0-1.3$ plus reflection from a cold or mildly ionized slab with a covering factor of $\Omega/2\pi \sim 0.2-0.3$. A soft excess below 10 keV, interpreted as emission from the accretion disk, is seen to decrease during the 1.5 months spanned by our observations. Our results indicate a remarkable consistency among the independently calibrated detectors, with the remaining issues being mainly related to the flux calibration of *INTEGRAL*.

Key words. black hole physics – stars: individual: Cyg X-1 – gamma rays: observations – X-rays: binaries – X-rays: general

1. Introduction

The broad band X-ray continuum of Galactic black holes (BH) in the hard state is characterized by a power-law with photon index $\Gamma \sim 1.7$, and an exponential cutoff at ~150 keV, which is generally attributed to Comptonization (Sunyaev & Trümper 1979). A soft excess below ~1 keV, a hardening above 10 keV attributed to Compton reflection, and a fluorescent 6.4 keV Fe Kα line are all taken as evidence for the presence of a (possibly mildly ionized) accretion disk. Long-term monitoring programs and the existence of state changes from the hard state to the soft state (see, e.g., Remillard 2001) show that the relative contribution of the Comptonizing medium and the accretion disk to the emitted X-ray luminosity are variable on long timescales (Pottschmidt et al. 2003; Zdziarski et al. 2002).

Send offprint requests to: K. Pottschmidt,
e-mail: `katja.pottschmidt@obs.unige.ch`

The knowledge of the spectral shape above 10 keV is crucial for the determination of the temperature and optical depth of the Comptonizing medium, as well as for the determination of the reflection fraction. With the launch of the *International Gamma-Ray Astrophysics Laboratory* (*INTEGRAL*), a new instrument providing data from 5 keV to several MeV has become available. To test the *INTEGRAL* instruments and further our knowledge of BH spectra, we organized simultaneous measurements of the canonical BH Cygnus X-1 with the *Rossi X-ray Timing Explorer* (*RXTE*) during *INTEGRAL*'s performance verification (PV) phase. Here, we present first results of these observations. In Sect. 2 we describe the observations and the data extraction, followed in Sect. 3 by the results of our modeling. Section 4 summarizes our main points.

2. Observations and data analysis

Cyg X-1 was observed during the PV phase of *INTEGRAL* in a variety of different observing modes. *RXTE* observing times were chosen to coincide with *INTEGRAL* observations that pointed at the source (satellite revolutions 11, 14, 16, and 18) as well as with observations during revolution 25,

Table 1. Log of the simultaneous *INTEGRAL/RXTE* observations, showing the *INTEGRAL* revolution (Rev.), the date of the observation, as well as the exposure time of the instruments used in the data analysis in ksec (for *RXTE*, we give the PCA exposure and the dead-time corrected HEXTE live-time).

Rev.	Date	*RXTE*	JEM X1	X2	ISGRI	SPI
11	2002-11-16	12.1/8.1	–	–	11.7	86.0
14	2002-11-26	6.7/4.1	–	15.0	0.6	–
16	2002-12-02	4.1/2.6	–	10.1	5.8	–
18	2002-12-06	7.5/5.2	10.6	–	12.2	–
25	2002-12-29	29.7/34.9	–	–	8.0	86.4

where Cyg X-1 was on average ~10° off-axis. During revolutions 14, 16, and 18 *INTEGRAL* performed staring observations dedicated to the calibration of the Joint European X-ray Monitor (JEM-X; Lund et al. 2003) and the Imager on-board *INTEGRAL* (IBIS; Ubertini et al. 2003). For both instruments, data simultaneous to *RXTE* were extracted on "science window timescales" (i.e., stable *INTEGRAL* pointings of ~2000 s length). For these revolutions, no source spectrum could be extracted from the Spectrometer on-board *INTEGRAL* (SPI; Vedrenne et al. 2003), as *INTEGRAL* was not in one of its dithering modes and the SPI imaging solution is underdetermined. Information from SPI is only available for the hexagonal dithering mode in revolution 11 and for the 5×5 dither pattern of revolution 25 (see Courvoisier et al. 2003 for a description of *INTEGRAL*'s dithering patterns). Due to the small effective area of SPI, we use data from the whole *INTEGRAL* revolution contemporaneous to the *RXTE* observations. For the IBIS analysis of these two revolutions, only the closest contemporaneous science windows were considered. These were either on-axis (rev. 11) or had an offset of <5° (rev. 25). The JEM-X data extraction failed for these two revolutions. Table 1 provides a log of all the observations analyzed herein. See Bazzano et al. (2003) for discussions of (non-simultaneous with *RXTE*) IBIS data of Cyg X-1.

The *INTEGRAL* data were extracted using the *INTEGRAL* off-line scientific analysis (OSA) software, version 1.1, including those fixes to the released software which were available up to 2003 June 15. For all instruments, the newest available response matrices were used. Data from JEM-X were considered from 10–40 keV only, due to on-board event selection effects in the early phase of the mission (before rev. 45). For IBIS we used data from 40–250 keV, the energy band in which the energy response of IBIS was considered calibrated at the time of writing, and only considered the *INTEGRAL* Soft Gamma-Ray Imager (ISGRI) part of the detector. We applied the 10% systematic uncertainty recommended by the IBIS team (Ubertini, priv. comm.) in quadrature to the data. For SPI, data from 50–200 keV were extracted with SPIROS, version 4.3.4 (Skinner & Connell 2003; Strong 2003). See Sect. 3 for a discussion of this rather low upper energy threshold of SPI. For all instruments, background subtraction has been taken into account by the OSA. Current experience shows, e.g., that with ISGRI a few ks are sufficient to extract a significant spectrum up to ~100 keV for a 60 mCrab source (Paizis et al. 2003),
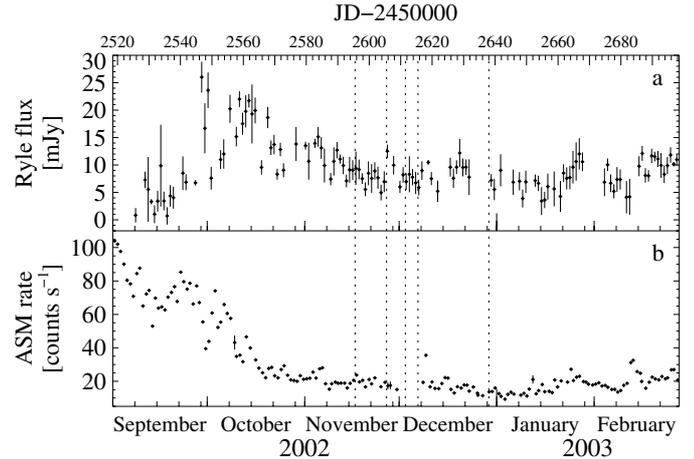

Fig. 1. a) 15 GHz radio lightcurve from the Ryle telescope and **b)** 2–12 keV *RXTE*-All Sky Monitor flux of Cyg X-1 for the time of the pointed *INTEGRAL* and *RXTE* observations (dashed lines). Note the end of the 2002 soft state of Cyg X-1 in 2002 mid-October.

thus background influences should not be an issue for Cyg X-1 up to a few 100 keV.

We compare the *INTEGRAL* data with measurements from both *RXTE* pointed instruments, the Proportional Counter Array (PCA; Jahoda et al. 1997) and the High Energy X-ray Timing Experiment (HEXTE; Rothschild et al. 1998). The *RXTE* data were extracted with the HEASOFT software, version 5.2, using our standard procedures (e.g., Wilms et al. 1999). The high effective area of the PCA (~4000 cm^2) necessitates the use of energy dependent systematic uncertainties of 1% for PCA channels 0–15 ($\lesssim$7.5 keV), 0.5% for channels 16–39 (7.5 keV–18 keV), and 2% up to 25 keV (Kreykenbohm et al. 2003). These uncertainties are added in quadrature to the data. For the HEXTE, the 20 keV–200 keV energy range was considered. Finally, the Ryle telescope in Cambridge, England, performed simultaneous radio observations at 15 GHz in addition to its daily monitoring of the source (Fig. 1).

Spectral fitting was performed with XSPEC 11.2.0bc (Arnaud 1996), which includes important fixes to the reflection model used in the spectral analysis (Sect. 3). The uncertainty of the instrument flux calibration was taken into account by introducing a multiplicative constant into the spectral models, and normalizing all fluxes to the PCA. This constant was 0.80–0.84 for the HEXTE (consistent with earlier results), 0.56 for JEM-X1, 0.43 and 0.46 for JEM-X2, 1.03 and 1.05 for SPI, and it varied between 0.89 and 1.38 for ISGRI (see Tables 2 and 3 below). The latter large variation is mainly due to known issues with the current ISGRI deadtime correction.

3. Modeling the 3–250 keV spectrum

We modeled the spectra using the canonical model for the hard state, a Comptonization continuum which is partly reflected off a slab-like accretion disk. In these models, it is assumed that the Comptonizing medium sandwiches the accretion disk, although its covering factor can be less than unity. This geometry is not the only possible one for Cyg X-1. Sphere+disk models, e.g., where the Comptonizing medium is an inner spherical

Table 2. Best fit parameters for the `compTT` model (full model in XSPEC notation: const×phabs[diskbb+gauss+compTT+reflect (comptt)]). The parameters shown are the inner accretion disk temperature kT_{in} and its normalization, $A_{disk} = ((R_{in}/km)/(D/10\,kpc))^2 \cos i$, the electron temperature of the Comptonizing plasma, kT_e and its optical depth τ, the covering factor of the cold reflecting medium, $\Omega/2\pi$, and the energy and width of the Gaussian Fe Kα line, $E_{K\alpha}$ and $\sigma_{K\alpha}$, and the flux normalization constants of the individual instruments with respect to the PCA are given by c_{HEXTE}, c_{ISGRI}, c_{JEM-X1}, c_{JEM-X2}, and c_{SPI}. For revolutions 11 and 25 the results are shown with and without taking SPI into account in order to illustrate its systematic influences.

	Rev. 11	Rev. 14	Rev. 16	Rev. 18	Rev. 25	Rev. 11 SPI	Rev. 25 SPI
kT_{in} [eV]	735^{+77}_{-113}	745^{+102}_{-162}	710^{+72}_{-122}	772^{+90}_{-157}	660^{+65}_{-143}	670^{+87}_{-90}	651^{+75}_{-119}
A_{disk}	540^{+790}_{-200}	460^{+1140}_{-190}	440^{+800}_{-150}	430^{+820}_{-150}	260^{+300}_{-80}	650^{+120}_{-50}	270^{+450}_{-90}
kT_e [keV]	62^{+7}_{-8}	54^{+7}_{-4}	62^{+19}_{-9}	51^{+3}_{-3}	62^{+4}_{-4}	252^{+26}_{-32}	94^{+39}_{-20}
τ	$1.01^{+0.15}_{-0.11}$	$1.21^{+0.09}_{-0.13}$	$1.06^{+0.17}_{-0.26}$	$1.24^{+0.07}_{-0.07}$	$1.07^{+0.08}_{-0.06}$	$0.16^{+0.05}_{-0.04}$	$0.69^{+0.20}_{-0.17}$
$\Omega/2\pi$	$0.17^{+0.01}_{-0.01}$	$0.17^{+0.01}_{-0.01}$	$0.19^{+0.01}_{-0.02}$	$0.19^{+0.01}_{-0.01}$	$0.17^{+0.01}_{-0.01}$	$0.24^{+0.01}_{-0.01}$	$0.17^{+0.00}_{-0.00}$
$E_{K\alpha}$ [keV]	$6.42^{+0.22}_{-0.39}$	$6.28^{+0.31}_{-0.65}$	$6.38^{+0.25}_{-0.49}$	$6.24^{+0.25}_{-0.54}$	$6.13^{+0.27}_{-0.35}$	$6.44^{+0.13}_{-0.13}$	$6.10^{+0.30}_{-0.28}$
$\sigma_{K\alpha}$ [keV]	$0.74^{+0.32}_{-0.31}$	$0.86^{+0.41}_{-0.39}$	$0.66^{+0.39}_{-0.35}$	$0.78^{+0.39}_{-0.35}$	$0.59^{+0.32}_{-0.31}$	$0.61^{+0.15}_{-0.14}$	$0.62^{+0.31}_{-0.32}$
c_{HEXTE}	$0.83^{+0.01}_{-0.00}$	$0.81^{+0.01}_{-0.01}$	$0.80^{+0.01}_{-0.01}$	$0.84^{+0.01}_{-0.01}$	$0.83^{+0.01}_{-0.00}$	$0.82^{+0.00}_{-0.00}$	$0.83^{+0.00}_{-0.00}$
c_{ISGRI}	$1.08^{+0.05}_{-0.05}$	$0.89^{+0.06}_{-0.06}$	$1.36^{+0.06}_{-0.07}$	$1.38^{+0.05}_{-0.06}$	$1.23^{+0.05}_{-0.05}$	$1.01^{+0.04}_{-0.04}$	$1.21^{+0.05}_{-0.05}$
c_{JEM-X1}	–	–	–	$0.560^{+0.004}_{-0.004}$	–	–	–
c_{JEM-X2}	–	$0.456^{+0.003}_{-0.003}$	$0.428^{+0.004}_{-0.004}$	–	–	–	–
c_{SPI}	–	–	–	–	–	$1.05^{+0.00}_{-0.01}$	$1.03^{+0.01}_{-0.01}$
χ^2/d.o.f.	228/240	321/317	387/318	352/339	505/240	413/279	589/253
χ^2_{red}	0.95	1.01	1.22	1.04	2.11	1.48	2.33

Table 3. Best fit parameters for the `eqpair` fits (full model in XSPEC notation: const×phabs[diskbb+gauss+eqpair]). Shown are the disk parameters kT_{in} and A_{disk}, inner accretion disk temperature, kT_{in}, the ratio of the compactness of the Comptonizing plasma to the accretion disk compactness, l_h/l_s, from which the Comptonization temperature kT_e can be derived (as kT_e is not a fit parameter, we do not give its uncertainty), the optical depth of the Comptonizing plasma, τ, the covering factor of the reflecting medium, $\Omega/2\pi$, and its ionization parameter, ξ, the energy $E_{K\alpha}$ and width σ of the Fe Kα line (where $E_{K\alpha}$ was limited to ≥ 6 keV in the fits), and the flux normalization constants of the instruments with respect to the PCA. As in Table 2, for revolutions 11 and 25 the results are shown with and without taking SPI into account.

|	Rev. 11	Rev. 14	Rev. 16	Rev. 18	Rev. 25	Rev. 11 SPI	Rev. 25 SPI
kT_{in} [eV]	256^{+1}_{-5}	250^{+5}_{-8}	249^{+6}_{-8}	251^{+5}_{-6}	274^{+9}_{-44}	258^{+3}_{-7}	254^{+25}_{-29}
$A_{disk}/10^5$	36^{+8}_{-7}	32^{+9}_{-9}	23^{+9}_{-9}	34^{+5}_{-9}	0^{+1}_{-0}	38^{+6}_{-7}	0^{+2}_{-0}
l_h/l_s	$9.0^{+0.1}_{-0.1}$	$10.0^{+0.1}_{-0.1}$	$10.0^{+0.2}_{-0.1}$	$9.7^{+0.1}_{-0.1}$	$10.2^{+0.1}_{-0.1}$	$8.8^{+0.1}_{-0.1}$	$10.5^{+0.1}_{-0.2}$
kT_e [keV]	85	85	85	73	89	146	89
τ	$1.29^{+0.03}_{-0.03}$	$1.33^{+0.02}_{-0.04}$	$1.33^{+0.05}_{-0.06}$	$1.52^{+0.01}_{-0.01}$	$1.31^{+0.02}_{-0.02}$	$0.75^{+0.01}_{-0.03}$	$1.30^{+0.01}_{-0.02}$
$\Omega/2\pi$	$0.26^{+0.01}_{-0.01}$	$0.25^{+0.01}_{-0.01}$	$0.27^{+0.02}_{-0.01}$	$0.26^{+0.01}_{-0.01}$	$0.28^{+0.01}_{-0.01}$	$0.28^{+0.01}_{-0.01}$	$0.28^{+0.01}_{-0.01}$
ξ	89^{+11}_{-49}	0^{+4}_{-0}	43^{+53}_{-38}	0^{+8}_{-0}	32^{+23}_{-16}	0^{+22}_{-0}	32^{+21}_{-17}
$E_{K\alpha}$ [keV]	$6.00^{+0.11}_{-0.00}$	$6.00^{+0.07}_{-0.00}$	$6.00^{+0.53}_{-0.00}$	$6.00^{+2.00}_{-0.00}$	$6.29^{+0.24}_{-0.29}$	$6.00^{+0.03}_{-0.00}$	$6.30^{+0.24}_{-0.30}$
$\sigma_{K\alpha}$ [keV]	$0.86^{+0.19}_{-0.29}$	$0.98^{+0.14}_{-0.14}$	$0.78^{+0.30}_{-0.73}$	$0.92^{+1.15}_{-0.13}$	$0.29^{+0.40}_{-0.29}$	$1.00^{+0.06}_{-0.16}$	$0.29^{+0.40}_{-0.29}$
c_{HEXTE}	$0.84^{+0.00}_{-0.18}$	$0.82^{+0.01}_{-0.14}$	$0.82^{+0.01}_{-0.14}$	$0.85^{+0.10}_{-0.00}$	$0.82^{+0.00}_{-0.00}$	$0.83^{+0.00}_{-0.00}$	$0.82^{+0.15}_{-0.00}$
c_{ISGRI}	$1.10^{+0.05}_{-0.04}$	$0.90^{+0.06}_{-0.06}$	$1.38^{+0.06}_{-0.06}$	$1.39^{+0.05}_{-0.05}$	$1.23^{+0.05}_{-0.05}$	$1.03^{+0.04}_{-0.04}$	$1.23^{+0.05}_{-0.05}$
c_{JEM-X1}	–	–	–	$0.561^{+0.004}_{-0.004}$	–	–	–
c_{JEM-X2}	–	$0.456^{+0.003}_{-0.003}$	$0.429^{+0.004}_{-0.004}$	–	–	–	–
c_{SPI}	–	–	–	–	–	$1.06^{+0.01}_{-0.01}$	$1.04^{+0.01}_{-0.01}$
χ^2/d.o.f.	246/239	335/316	380/317	370/338	406/239	440/278	509/252
χ^2_{red}	1.03	1.06	1.20	1.10	1.70	1.58	2.02
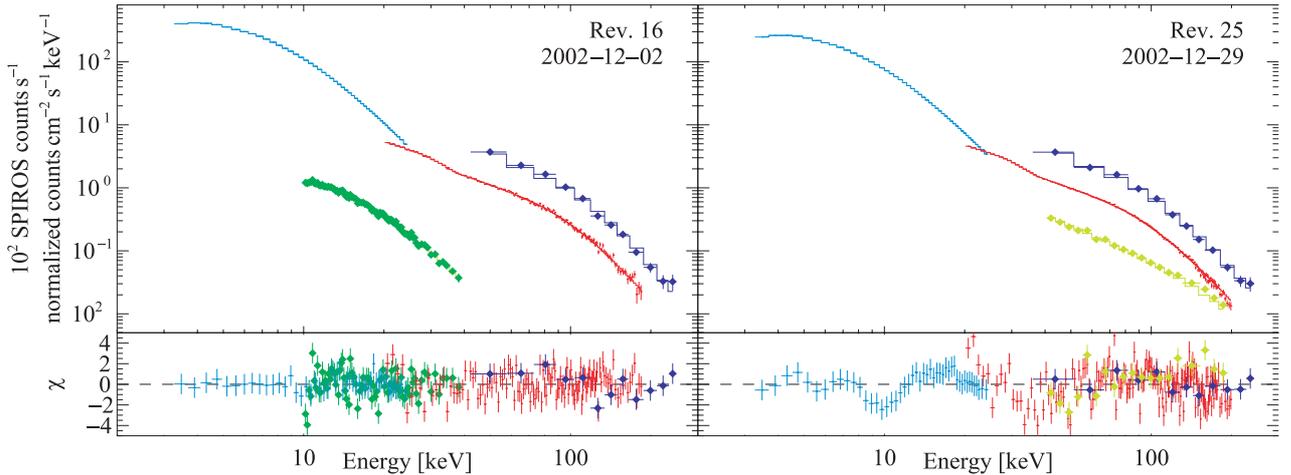
Fig. 2. Spectra, best fit `compTT` model, and residuals for the observations of 2002 December 02 and 2002 December 29 (PCA, 3–25 keV, light blue; JEM-X, 10–40 keV, green; HEXTE, 20–200 keV, red; IBIS, 40–250 keV, dark blue; SPI, 50–200 keV, olive green). For SPI, the spectrum as provided by the SPI spectral extractor, SPIROS, is shown, for the other instruments, we display the count rate normalized by the detector effective area. The PCA residuals for revolution 25 are consistent with known systematic effects.
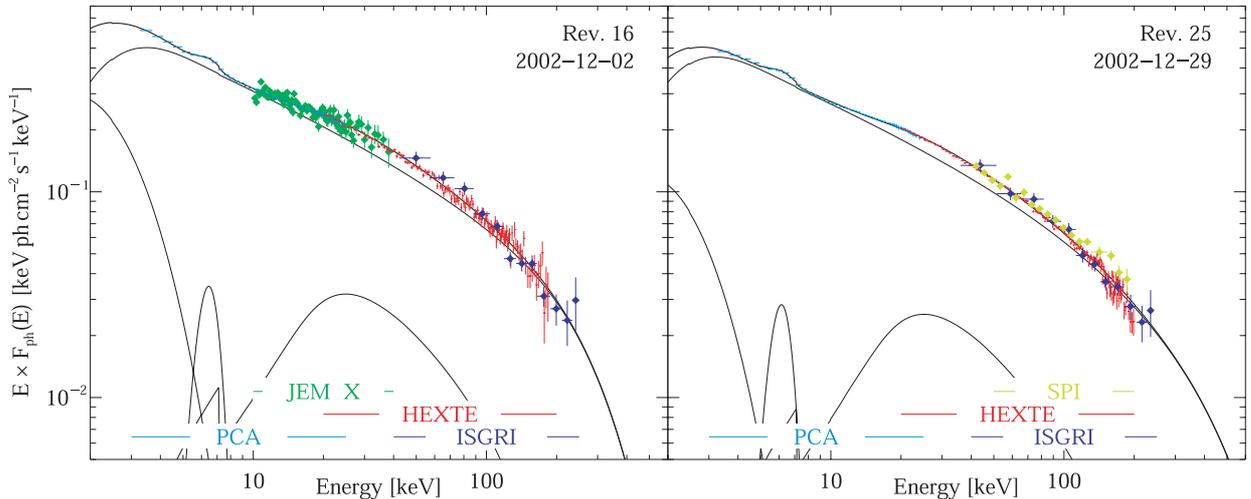
Fig. 3. Unfolded X-ray spectra for the observations of Fig. 2, and the components of the `compTT` model. For all instruments, the measured fluxes have been renormalized to that measured by the PCA, the colors are those of Fig. 2.

accretion flow irradiated by an outer accretion disk (possibly slightly penetrating the sphere) have also been shown to describe the data (Dove et al. 1997, 1998; Zdziarski et al. 1999). Furthermore, emission from the base of a jet might also contribute to the observed X-rays (Markoff et al. 2002). We will consider such more complex models in a future paper.

Due to the limitations intrinsic to the available Comptonization models, it is generally useful to apply several different Comptonization models to the data. Such an approach allows one to test whether any trends seen in the evolution of spectral fit parameters are stable against these limitations. See, e.g., Nowak et al. (2002) for a discussion of these issues in the context of *RXTE* observations of GX 339−4. We therefore describe our joint *INTEGRAL-RXTE* spectra using two different kinds of spectral models. The first one is based on the theory of Hua & Titarchuk (1995, XSPEC model `compTT`) as a Comptonization continuum, which assumes a Wien spectrum for the seed photons. This continuum is

then partly reflected off a cold accretion disk (Magdziarz & Zdziarski 1995). To account for the effects of a patchy Comptonizing plasma, an additional soft disk black body (Mitsuda et al. 1984) is added. The temperature at the inner edge of the disk, kT_{in}, is set equal to the seed photon temperature. As the reflection model does not include fluorescent line emission, the Fe Kα line at 6.4 keV is described by a Gaussian. We also use a fixed absorbing column of $N_{H} = 6 \times 10^{21}$ cm^{-2} (Bałucińska-Church et al. 1995), as the PCA 3 keV lower threshold does not allow such low columns to be constrained.

We also described our data using the thermal Comptonization model of Coppi (1999, XSPEC model-name `eqpair`)[1], which includes reflection off a possibly ionized accretion disk (Magdziarz & Zdziarski 1995; Done et al. 1992). In this case, the spectral shape of the seed photons is a disk black body, part of which is not Comptonized to

---

[1] The `eqpair`-model is available as a local XSPEC model at http://www.astro.yale.edu/coppi/

take into account the possibility of a patchy Compton corona. This has again been realized in form of an additional disk black body component of the same temperature as the seed photons. The Fe Kα line is again described by a Gaussian and absorption is treated identical as in the compTT fits.

Both models resulted in equally good descriptions of the data. We show examples of our best fits in Figs. 2 and 3, and list the best fit parameters for all observations in Tables 2 and 3. For revolution 25, $\chi^2_{\rm red} = 2.1$, for the other observations $\chi^2_{\rm red} < 1.5$. Due to the long PCA exposure of rev. 25, χ^2 is dominated by the PCA (the PCA residuals shown for revolution 25 in Fig. 2 are consistent with calibration uncertainties). We therefore conclude that all of our Comptonization fits resulted in a satisfactory description of the 3–200 keV data from Cyg X-1.

For the compTT model, the Comptonization parameters are in principle consistent with earlier observations (Dove et al. 1998; Gierliński et al. 1997). For all five observations, the Comptonization temperature lies between 50 and 60 keV and the Thomson optical depth of the corona between 1 and 1.2 (cf. the two last columns of Table 2 for systematic influences from the SPI spectrum). These parameters vary only slightly with time, as is expected for the hard state of Cyg X-1. The covering factor of the reflecting slab is $\Omega/2\pi \sim 0.18$. This rather small value could imply that the Compton corona only covers part of the accretion disk, or that the accretion geometry is more complicated than the slab geometry assumed here (sphere+disk models, e.g., imply $\Omega/2\pi \lesssim 0.3$; Dove et al. 1997). The eqpair models agree qualitatively with these results and also require moderate τ and $\Omega/2\pi < 0.5$. They also allow for a very modest amount of ionization, with ionization parameters $\xi \lesssim 100$. For both, compTT and eqpair, iron lines were consistent with equivalent widths of ~50 to 100 eV, and are possibly broad.

Contrary to this constant behavior above 10 keV, the spectrum is much more variable on the long term at lower energies (e.g., Zdziarski et al. 2002, Fig. 12). Here we see a systematic evolution of the soft X-ray spectrum. For the compTT model fits, the flux of the non-Comptonized disk component decreases by a factor of about two between the first and the last of our observations, whereas for the eqpair fits, the flux of the additional disk component nearly completely vanishes. It is tempting to interpret this decrease in the flux of the soft model component as a true physical indication of the final stages of the 2002 transition out of the soft state, given the proximity of our first observation to the end of this state (Fig. 1).

The temperature of the non-Comptonized disk component is rather high for the compTT fits ($kT_{\rm in} \sim 700$ eV, implying an inner disk radius comparable to that of the last marginally stable orbit of a disk around a $10 M_\odot$ Schwarzschild black hole). There have been reports of a soft excess in the hard state of Cyg X-1 in addition to the black body provided by the disk (e.g., Di Salvo et al. 2001) and the hard Comptonized component. In principle, such an excess might explain our compTT parameters, however, our data do not allow to evaluate more complex models for the soft energy regime. Also, the disk temperature found in the eqpair fits is significantly lower. Here it is close to the $kT_{\rm in} = 200$ eV found, e.g., with ROSAT (Bałucińska-Church et al. 1995), with an implied disk radius near $50 GM/c^2$ for a $10 M_\odot$ BH. The Fe Kα line energy in the

eqpair fits is systematically too low, however, possibly indicating the soft spectral complexity noted above.

This discrepancy of the temperatures and implied disk radii might be caused by slight differences in the treatment of the transition of the seed photon spectrum to the Comptonization spectrum, especially given that compTT describes the seed photons with a simple Wien spectrum. Note also that constraining the temperature of the disk black body component to the seed photon temperature – a rather established simplification – removes some degeneracy from the low energy parameters. Finally, we also cannot exclude the possibility that part of the fitted black body is due to the calibrations of the PCA below ~10 keV, especially given that the temperatures of the soft components for both cases, compTT and eqpair fits, imply the peak emission is falling below the ~3 keV lower cutoff of the PCA. We conclude that our simplifications of the low energy spectral model are justified, especially since their effect on the parameters derived for the spectrum above 10 keV can be expected to be negligible. Note that the spectral shapes measured above 10 keV band with the PCA, HEXTE, JEM-X, and ISGRI are indeed remarkably consistent with each other, suggesting that their respective calibrations are in agreement.

Measurements with the Compton Gamma-Ray Observatory (CGRO) and *RXTE* show the presence of a hard tail from non-thermal Comptonization at $\gtrsim 300$ keV in the hard state of Cyg X-1 and above several keV in the soft state (Gierliński et al. 1999; McConnell et al. 2000, 2002). In principle, ISGRI and SPI detect Cyg X-1 to at least 500 keV and should be able to detect significantly this hard tail. Currently, however, the intercalibration of the instruments above 250 keV is not yet good enough to allow an extrapolation to this energy band. While ISGRI and HEXTE are in good agreement, showing a spectral turnover and having a peak of νf_ν at ~100 keV, the SPI spectrum is consistent with a continuation of a pure power-law.

4. Conclusions

We have presented first results from fitting simultaneous *INTEGRAL-RXTE* data of Cyg X-1 with two different Comptonization models. Our results for the spectral shape are in basic agreement with earlier results, with HEXTE, ISGRI, JEM-X, and to a lesser extent SPI, agreeing with each other. We take this result to mean that the energy redistribution of the *INTEGRAL* instruments is well understood up to ~250 keV. The flux normalizations of the instruments, however, still show large deviations among instruments. This is likely caused by insufficient modeling of the instrumental deadtimes, the deconvolution of the coded mask images, and the calibration of the off-axis effective area.

The high total signal above 10 keV in principle allows us to constrain the continuum shape to a higher degree than has been possible with *RXTE* or *BeppoSAX* alone. The presence of an additional, comparatively weak Comptonized component cannot be constrained. In two of the reported cases the additional Comptonized component peaks at ~1 keV, and thus only affects the spectrum at $\lesssim 10$ keV (Di Salvo et al. 2001; Frontera et al. 2001, *BeppoSax* data). *Ginga* and *OSSE* data

Letter to the Editor

were analyzed using different Comptonization models from those applied here and direct comparisons cannot be made (Gierliński et al. 1997, $kT_1 \sim 110$ keV, $\tau_1 \sim 1.7$, $kT_2 \sim 45$ keV, $\tau_2 \sim 6$). Interestingly, the use of a directly comparable approach (Maccarone & Coppi 2003, `eqpair`, *RXTE/OSSE* data) also results in a good spectral description using a single thermal Comptonization component and parameters fully consistent with our non-SPI fits. This might indicate a good stability of the hard state spectral shape above 10 keV on a time scale of years.

Thus it is quite clear that apart from model details our overall description of the hard state spectrum above 10 keV – i.e., with thermal Comptonization and a covering factor of the reflector of $\Omega/2\pi < 0.3$ – is principally the same as found previously (Dove et al. 1998; Gierliński et al. 1997; Di Salvo et al. 2001; Frontera et al. 2001; Maccarone & Coppi 2003). Comptonization plus reflection models, featuring a partial covering of the reflector or a geometrically more complicated accretion disk configuration, are thus still feasible explanations of the X-ray spectrum. Direct comparisons between these models and other alternative explanations, e.g., involving jet physics, still need to be performed. The decrease of the observed black body flux in the PCA data could be caused by the accretion disk fading away after the 2002 soft state.

We stress that this paper only contains the preliminary fits employing the earliest available response models for *INTEGRAL*. These models, however, already show a remarkable consistency among independent detectors over a range from 10–200 keV, with the remaining issues being mainly related to the flux calibration of *INTEGRAL*. Despite these limitations we have shown that Comptonization models already provide a good description of the joint 3–250 keV *INTEGRAL-RXTE* data. As the calibration of *INTEGRAL* improves, tests using more advanced models than those employed here will become possible. Since the *INTEGRAL* data will cover the important range above 250 keV, where Klein-Nishina effects become important for the shape of the Comptonization continuum and where the non-thermal tails start to dominate, it is expected in the near future that these data will allow us to constrain the important physical parameters responsible for the generation of the X-ray spectrum of the hard state of Galactic black holes.

References

Arnaud, K. A. 1996, in Astronomical Data Analysis Software and Systems V, ed. J. H. Jacoby, & J. Barnes (San Francisco: Astron. Soc. Pacific), ASP Conf. Ser., 101, 17

Bałucińska-Church, M., Belloni, T., Church, M. J., & Hasinger, G. 1995, A&A, 302, L5

Bazzano, A., Bird, A., Capitanio, F., et al. 2003, A&A, 411, L389

Coppi, P. 1999, in High Energy Processes in Accreting Black Holes, ed. J. Poutanen, & R. Svensson (San Francisco: Astron. Soc. Pacific), ASP Conf. Ser. 161, 375

Courvoisier, T. J.-L., Walter, R., Beckmann, V., et al. 2003, A&A, 411, L53

Di Salvo, T., Done, C., Życki, P. T., Burderi, L., & Robba, N. R. 2001, ApJ, 547, 1024

Done, C., Mulchaey, J. S., Mushotzky, R. F., & Arnaud, K. A. 1992, ApJ, 395, 275

Dove, J. B., Wilms, J., Maisack, M. G., & Begelman, M. C. 1997, ApJ, 487, 759

Dove, J. B., Wilms, J., Nowak, M. A., Vaughan, B., & Begelman, M. C. 1998, MNRAS, 289, 729

Frontera, F., Palazzi, E., Zdziarski, A. A., et al. 2001, ApJ, 546, 1027

Gierliński, M., Zdziarski, A. A., Done, C., et al. 1997, MNRAS, 288, 958

Gierliński, M., Zdziarski, A. A., Poutanen, J., et al. 1999, MNRAS, 309, 496

Hua, X.-M., & Titarchuk, L. 1995, ApJ, 449, 188

Jahoda, K., Swank, J. H., Giles, A. B., et al. 1997, in EUV, X-Ray, and Gamma-Ray Instrumentation for Astronomy VII, ed. O. H. Siegmund (Bellingham, WA: SPIE), Proc. SPIE, 2808, 59

Kreykenbohm, I., Wilms, J., Coburn, W., et al. 2003, A&A, submitted

Lund, N., Brandt, S., Budtz-Jørgensen, C., et al. 2003, A&A, 411, L231

Maccarone, T. J., & Coppi, P. S. 2003, MNRAS

Magdziarz, P., & Zdziarski, A. A. 1995, MNRAS, 273, 837

Markoff, S., Nowak, M., Corbel, S., Fender, R., & Falcke, H. 2002, A&A, 397, 645

McConnell, M. L., Ryan, J. M., Collmar, W., et al. 2000, ApJ, 543, 928

McConnell, M. L., Zdziarski, A. A., Bennett, K., et al. 2002, ApJ, 572, 984

Mitsuda, K., Inoue, H., Koyama, K., et al. 1984, PASJ, 36, 741

Nowak, M. A., Wilms, J., & Dove, J. B. 2002, MNRAS, 332, 856

Paizis, A., Beckmann, V., Courvoisier, T. J.-L., et al. 2003, A&A, 411, L363

Pottschmidt, K., Wilms, J., Nowak, M. A., et al. 2003, A&A, 407, 1039

Remillard, R. A. 2001, in Evolution of Binary and Multiple Stars, ed. P. Podsiadlowski, S. Rappaport, A. King, F. D'Antona, & L. Burderi (San Francisco), ASP Conf. Proc., 229, 503

Rothschild, R. E., Blanco, P. R., Gruber, D. E., et al. 1998, ApJ, 496, 538

Skinner, G., & Connell, P. 2003, A&A, 411, L123

Strong, A. 2003, A&A, 411, L127

Sunyaev, R. A., & Trümper, J. 1979, Nature, 279, 506

Ubertini, P., Lebrun, F., Di Cocco, G., et al. 2003, A&A, 411, L131

Vedrenne, G., Roques, J.-P., Schönfelder, V., et al. 2003, A&A, 411, L63

Wilms, J., Nowak, M. A., Dove, J. B., Fender, R. P., & di Matteo, T. 1999, ApJ, 522, 460

Zdziarski, A. A., Lubiński, P., & Smith, D. A. 1999, MNRAS, 303, L11

Zdziarski, A. A., Poutanen, J., Paciesas, W. S., & Wen, L. 2002, ApJ, 578, 357